

p - ^4He scattering: New data and a phase-shift analysis between 30 and 72 MeV

S. Burzynski

Institute for Nuclear Studies, Hoza 69, Warsaw, Poland

J. Campbell, M. Hammans, R. Henneck, W. Lorenzon, M. A. Pickar,* and I. Sick

Institut für Physik, University of Basel, CH-4056 Basel, Switzerland

(Received 9 May 1988)

We have measured the differential cross section $d\sigma/d\Omega$ and the analyzing power A_y in the elastic p - ^4He scattering at 71.9 MeV. These data, together with all other existing data between 30 and 65 MeV, were subjected to a phase-shift analysis. New fixed energy solutions were found, which typically exhibit lower χ^2 values than existing solutions and are consistent with a continuous energy dependence. An energy-dependent analysis with a quadratic energy dependence reproduced the trend of the single-energy solutions, but yielded large χ^2 values.

I. INTRODUCTION

The elastic scattering of protons from ^4He in the energy range 20–65 MeV has been studied by several groups over the last three decades (cf. Ref. 1–3). As a result, good quality data for the differential cross section $d\sigma/d\Omega$ (with typical uncertainties of $\leq 2\%$ in statistics and $\leq 3\%$ in normalization) and for the analyzing power A_y (with uncertainties of ≤ 0.02 in statistics and normalization) have become available at energies which are spaced by no more than ~ 6 MeV. These data are supplemented by measurements of the total reaction cross section σ_R between 24 and 55 MeV (Ref. 2). In the lower-energy region several phase-shift analyses (PSA) were performed, of which the ones of Plattner *et al.*¹ and Houdayer *et al.*² are the most comprehensive. Plattner analyzed data of $d\sigma/d\Omega$ and A_y between 20 and 40 MeV, including few σ_R data near the threshold at 23 MeV. The phase shifts (PS) were found to be remarkably smooth in energy, except for two phenomena: an anomaly in the $^2D_{3/2}$ phase shift at 23.4 MeV, which corresponds to the well-known second excited state of ^3Li at 16.7 MeV and an indication of a structure in a few PS around 30 MeV, which supposedly originate from higher excitations of ^3Li (see, however, our conclusions herein). The finding that the absorption takes place predominantly in the even partial waves indicated, on the other hand, that the scattering process is not purely potential scattering. Both findings may be reconciled if one assumes the higher excitations to be broad, overlapping levels. Strong support for this argument has come from the study of deuteron-induced reactions on ^3He and ^3H and from cluster model calculations (cf. Refs. 1, 2, and references therein). The PSA of Houdayer² employed newly measured $d\sigma/d\Omega$ and σ_R data, the A_y data of Ref. 1 and some low quality, incomplete sets of A_y between 40 and 55 MeV. Using Plattner's solutions as starting values, their PSA is more or less identical to Plattner's up to 40 MeV. Above 40 MeV their solutions exhibit more scatter as a function of energy, but in general follow the trend of the lower-energy solutions. This is in marked contrast to

the most recent PSA by Saito,³ who analyzed new, accurate measurements of $d\sigma/d\Omega$ and A_y (Ref. 4) together with the σ_R data of Ref. 2 and σ_R predictions between 45 and 65 MeV. Saito found four sets of solutions over the whole energy range, of which two sets could be eliminated by including A_y data which were measured in the very forward-angle Coulomb interference region at 52 and 65 MeV (a region not spanned in any other A_y data). Compared to Houdayer's PSA both of Saito's solution sets are remarkably "unsmooth" in energy. The Houdayer PSA, on the other hand, failed to reproduce³ the analyzing powers of Ref. 4.

This quite unsatisfactory situation has prompted two new measurements: (i) the determination of the spin rotation parameter R at 65 MeV for angles up to 125° (Ref. 5) and (ii) a new, precise measurement of $d\sigma/d\Omega$ and A_y at 72 MeV, which is presented here.

The latter experiment was undertaken also for a second reason: in order to calibrate the polarization of a neutron beam, one usually takes advantage of the large analyzing power in n - ^4He elastic scattering at backangles (see, e.g., Ref. 6). This assumes that one can use the well-known analyzing powers of the p - ^4He elastic scattering, corrected for small Coulomb effects at backangles. In the approach of Ref. 7 this correction depends on the momentum derivatives of the PS. Since Saito's two solution sets differ in their energy dependence, the correction was also found to be significantly different.⁸ The "unsmooth" behavior of either set is indeed so strong that a reasonable extrapolation of the PS to an energy only 3 MeV above the highest energy yielded unrealistic values for A_y .

It is the purpose of this paper to present a new PSA in the energy range from 30 to 72 MeV. The main emphasis hereby was on the question, whether the scattering process can be described by smoothly energy dependent PS. In addition to the actual PSA, this required a detailed study of artificial data and of the uncertainties of the PS (this has not been done for the other PSA mentioned here). In the following, we shall first describe our experiment at 72 MeV and quote the results, then turn to the actual PSA and conclude with a discussion of our findings.

II. EXPERIMENT

Polarized protons from the Schweizerisches Institut für Nuklearforschung (SIN) injector cyclotron of (72.0 ± 0.2) MeV were focused into a polarimeter which is located upstream from the actual scattering chamber. The beam polarization was monitored continuously during the experiment via elastic proton scattering at 44.3° from a thin, natural carbon foil. After passing through the polarimeter, the beam was refocused into a scattering chamber of 1.2 m diameter, which contained a cooled gas target. The target consisted of a Cu cylinder of 60 mm diameter with $10 \mu\text{m}$ havar windows, which was clamped

tightly to the cold head of the refrigerator (Air Products CSW-208). The temperature was maintained at about 20 K by means of an external heat load, which was driven by a control unit (Air Products ADP-E, model 3700) in combination with a thermo couple attached to the cold head. A temperature sensitive diode (Lake Shore Cryotronics, DRC-7), clamped to the bottom of the target cylinder allowed us to monitor the temperature of the target to within 0.2 K. The target pressure was measured with a pressure gauge to within 10 mbars.

Scattering particles were observed in two ΔE - E -detector telescopes, which were usually placed symmetrically left and right with respect to the incident beam.

TABLE I. $d\sigma/d\Omega$ (cm) and A_y for p - ^4He elastic scattering at 71.9 MeV.

$\Theta_{\text{c.m.}}$	Θ_{lab}	$\frac{d\sigma}{d\Omega}$ (mb/sr)	$\Delta \frac{d\sigma}{d\Omega}$ (mb/sr)	A_y	ΔA_y
25.23	20.0	70.26	0.76	0.142	0.003
27.73	22.0	60.95	0.66	0.150	0.003
30.22	24.0	51.89	0.51	0.156	0.003
33.95	27.0	38.23	0.39	0.150	0.004
37.65	30.0	28.51	0.11	0.156	0.002
43.78	35.0	15.94	0.14	0.136	0.002
49.84	40.0	8.666	0.120	0.087	0.003
55.82	45.0	4.936	0.060	0.003	0.003
61.72	50.0	3.047	0.024	-0.102	0.003
67.54	55.0	2.127	0.015	-0.172	0.002
73.25	60.0	1.633	0.023	-0.196	0.003
78.86	65.0	1.299	0.024	-0.186	0.002
84.37	70.0	1.050	0.019	-0.156	0.003
89.76	75.0	0.8123	0.015	-0.110	0.003
95.04	80.0	0.6124	0.011	-0.063	0.004
100.20	85.0	0.4542	0.008	-0.023	0.005
102.23	87.0	0.3992	0.007	-0.000	0.003
104.25	89.0	0.3482	0.0066	0.011	0.004
105.24	90.0	0.3339	0.0054	0.012	0.003
107.23	92.0	0.2949	0.0060	0.021	0.006
110.17	95.0	0.2533	0.0045	0.016	0.004
114.98	100.0	0.1941	0.0035	-0.020	0.004
116.87	102.0	0.1758	0.0031	-0.045	0.004
119.67	105.0	0.1558	0.0028	-0.083	0.005
124.25	110.0	0.1296	0.0028	-0.090	0.009
126.05	112.0	0.1156	0.0025	-0.072	0.009
128.73	115.0	0.1109	0.0025	0.044	0.010
133.10	120.0	0.1009	0.0018	0.377	0.004
134.82	122.0	0.1039	0.0017	0.544	0.004
136.52	124.0	0.1217	0.0044	0.686	0.015
137.37	125.0	0.1172	0.0021	0.767	0.003
138.21	126.0	0.1225	0.0062	0.804	0.016
139.05	127.0	0.1332	0.0029	0.862	0.003
141.55	130.0	0.1687	0.0032	0.942	0.004
143.20	132.0	0.1954	0.0036	0.940	0.004
145.64	135.0	0.2542	0.0043	0.902	0.004
147.26	137.0	0.3004	0.0053	0.868	0.004
149.66	140.0	0.3749	0.0065	0.802	0.004
151.25	142.0	0.4353	0.0075	0.746	0.004
153.61	145.0	0.5343	0.009	0.667	0.004
157.49	150.0	0.7265	0.015	0.548	0.008
161.33	155.0	0.8999	0.020	0.429	0.009
165.12	160.0	1.064	0.023	0.327	0.008
168.87	165.0	1.324	0.027	0.251	0.007

Each telescope consisted of a 1 mm thick Si detector for ΔE measurement and a plastic scintillation detector. A double-slit collimation system in front of the telescopes subtended an angle range of 0.7° in the scattering plane. The characteristic length of the collimation system was $G_0 = 2.192 \mu\text{m}$ (Ref. 9). The collimator/detector assemblies were set to within 0.2° absolute by means of a telescope, which was aligned along the axis of the beam profile monitors. These beam profile monitors before and after the chamber were used to set up and monitor the beam during the experiment. The beam spot on target had a diameter of less than 4 mm. After passing through the chamber the beam was refocused into a Faraday cup with an electron suppressed graphite beam stop.

A. Data taking and results

1. Differential cross section $d\sigma/d\Omega$

All $p\text{-}^4\text{He}$ data were taken at about 20 K temperature and 1.5 bars pressure, which yields about 15 times higher density than at normal temperature and pressure (NTP). The proton energy at the center of the target was 71.9 MeV. In order to check on the performance of the temperature and pressure gauges, we also made some runs at room temperature. We observed a slight discrepancy between warm and cold yields, which is due to the fact that the temperature diode was not calibrated absolutely. The data were corrected for this discrepancy, which introduced a normalization uncertainty of 1%.

Empty target runs at several angles were used to check on the amount of background produced by scattering the beam halo from the windows. At forward angles we observed some background, which amounted to less than 0.1% of the $p\text{-}^4\text{He}$ events. Runs with different beam intensities at both room temperature and 20 K showed no indication of “beam heating,” i.e., local heating of the gas within the beam volume. This is important since data at forward angles were taken with intensities as low as 2 nA whereas at backangles up to 600 nA were used.

The data were corrected for a small Faraday cup bias current, as well as for the computer dead time of typically about 2%. The correction due to the inefficiency of the E detectors caused by inelastic reactions was made using the tables of Ref. 10. For several series of measurements at the same nominal angle but with typically slightly varying parameters (temperature, pressure, beam intensity, optics, and angle setting reproducibility) we observed a small nonstatistical variation of the yields, compatible with an overall relative uncertainty of $\sim 1\%$. This was taken as an upper limit for the systematic uncertainty. For part of the data ($\Theta_{\text{c.m.}} \geq 70^\circ$) the Faraday cup normalization was defective and these data were then normalized by means of the polarimeter integrated count rates. This introduced a relative uncertainty which had a statistical variation of 1.5%.

The $p\text{-}^4\text{He}$ yields were normalized to the yields obtained from pp scattering at the same energy. For that purpose the target was filled with hydrogen at room tem-

perature and about 1.2 bars pressure. The yields measured at several angles were normalized to “theoretical” yields as expected from Arndt’s 1985 50 MeV single-energy phase-shift solution¹¹ [this solution describes the existing cross-section data at 66.0 MeV (Ref. 12) and 68.3 MeV (Ref. 13) better than the 100 MeV single-energy solution or the global 0–1 GeV solution]. This way individual normalization factors for each detector were extracted. The comparison with the “theoretical” yields showed, that our data are statistically consistent with a relative accuracy of about 1.5%.

Table I shows the final results. The given uncertainties include the earlier discussed systematic effects as well as counting statistics, which are typically better than 0.5%. Figure 1 shows a logarithmic plot of the cross section together with a prediction of our PSA.

The absolute normalization depends mainly (apart from the earlier mentioned temperature correction uncertainty) on the accuracy of Arndt’s phase-shift prediction for pp scattering. Arndt’s code yields an error band of about 0.5%. However, since, e.g., the 66.0 MeV data¹² are underestimated by about 3%, whereas the 68.3 MeV data¹³ are well described, we believe the final absolute normalization to be good to within 2.5% (using the WI87

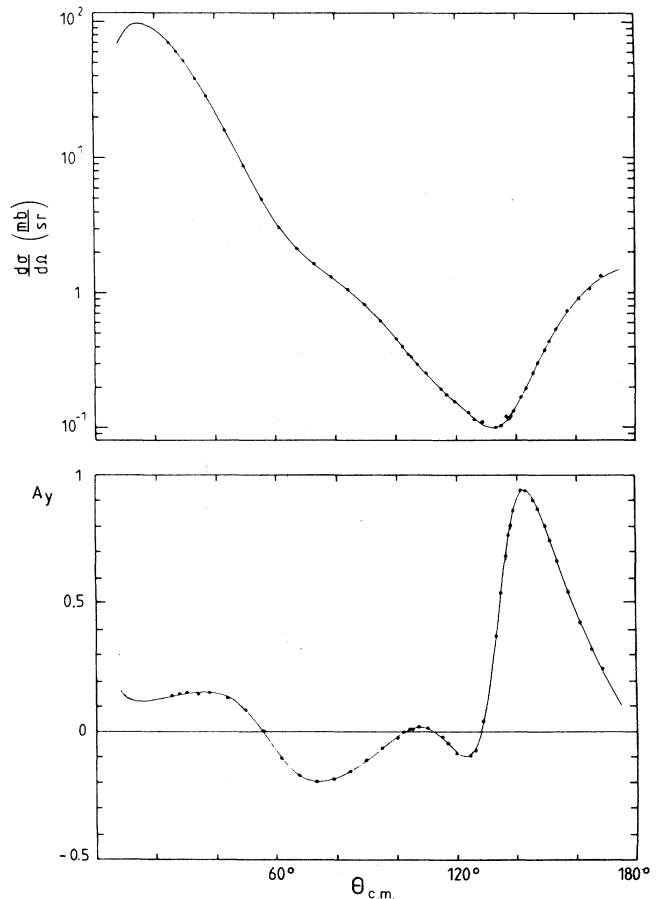


FIG. 1. The differential cross section $d\sigma/d\Omega$ and the analyzing power A_y as a function of $\Theta_{\text{c.m.}}$ at 71.9 MeV. The curve is our best-fit PS prediction.

50 MeV fixed energy phase-shift solution¹¹ would introduce a renormalization factor of 1.008, well within the stated uncertainty).

2. Analyzing powers

The analyzing power was extracted—whenever possible—using the symmetric setup of the two detectors by means of the super-ratio technique¹⁴

$$A_y \times P_y = \frac{r-1}{r+1}$$

and

$$r = \left(\frac{N_L^+ \times N_R^-}{N_L^- \times N_R^+} \right)^{1/2} . \quad (1)$$

Here, $N_L^\pm(N_R^\pm)$ refer to the dead-time corrected, normalized counts in the left (right) detector obtained with the + or - state of the beam polarization. The sign of the beam polarization was reversed every few seconds by switching rf transitions in the atomic-beam-type polarized ion source. Systematic contributions to $A_y P_y$ due to possible left/right asymmetries of the analyzing power, detector efficiency or solid angle and ΔP (see the following) were $\leq 5 \times 10^{-4}$ (Ref. 14). The beam polarization P_y —about ± 0.85 —was deduced from the polarimeter left/right count rates again using Eq. (1) and $A_y(72.0 \text{ MeV}, 44.3^\circ) = 0.966$ in p carbon scattering.¹⁵

For angles where only one detector could be used, the “single arm” analyzing power $A_L(A_R)$ was extracted using the relationship¹⁶

$$A_L = \frac{\epsilon_L}{P_y - \epsilon_L \times \Delta P} ,$$

where

$$\epsilon_L = \frac{N_L^+ - N_L^-}{N_L^+ + N_L^-} \quad (2)$$

and

$$\Delta P = \frac{P^+ + P^-}{2} .$$

$\Delta P \leq 0.001$ was extracted from the polarimeter data using the fact that the detectors were set at an angle where the p -carbon analyzing power has a maximum. For the cases where A_y could be determined via both methods (super ratio and single arm) the agreement was excellent.

A_y is listed in Table I together with its uncertainty, where we took into account small systematic variations, which were deduced from series of runs at the same nominal angle. Figure 1 shows a plot of A_y vs cm angle.

The absolute normalization of A_y hinges on the normalization of P_y , which in turn depends on the normalization of the measured analyzing power data in p -carbon scattering¹⁵ and on their interpolation at 71.9 MeV. Since Ref. 15 quotes ± 0.018 for the absolute normalization uncertainty and their statistical uncertainty in the maxima is typically ± 0.005 , we estimate the overall absolute uncertainty to be ± 0.02 .

III. PHASE-SHIFT ANALYSIS (PSA)

A. Formalism and search program

The expressions linking the observables $d\sigma/d\Omega$, A_y , and σ_R to the nuclear PS were taken from Ref. 3. The spin rotation parameter $R(\Theta)$ as a function of the laboratory scattering angle Θ was calculated from the following expression:

$$R(\Theta) = [(|g|^2 - |h|^2)\cos\Theta + 2\text{Re}(g \times h^*) \times \sin\Theta] / (|g|^2 + |h|^2) . \quad (3)$$

Here g and h are the nonspin-flip and spin-flip scattering amplitudes in spin $\frac{1}{2}$ on spin 0 elastic scattering. The analysis was carried out using a search routine which minimized the quantity χ_{tot}^2 ,

$$\chi_{\text{tot}}^2 = N_\sigma \times \chi_\sigma^2 + N_A \times \chi_A^2 + N_R \times \chi_R^2 + \chi_{\sigma_R}^2 + [(1-f_\sigma)/\Delta f_\sigma]^2 + [(1-f_A)/\Delta f_A]^2 + [(1-f_R)/\Delta f_R]^2 , \quad (4)$$

with

$$\begin{aligned} N_\sigma \times \chi_\sigma^2 &= \sum_{i=1}^{N_\sigma} [(\sigma_i^{\text{calc}} \times f_\sigma - \sigma_i^{\text{exp}}) / \Delta \sigma_i]^2 , \\ N_A \times \chi_A^2 &= \sum_{i=1}^{N_A} [(A_i^{\text{calc}} \times f_A - A_i^{\text{exp}}) / \Delta A_i]^2 , \\ N_R \times \chi_R^2 &= \sum_{i=1}^{N_R} [(R_i^{\text{calc}} \times f_R - R_i^{\text{exp}}) / \Delta R_i]^2 , \\ \chi_{\sigma_R}^2 &= [(\sigma_R^{\text{calc}} - \sigma_R^{\text{exp}}) / \Delta \sigma_R]^2 . \end{aligned}$$

The quantities χ_σ^2 , χ_A^2 , χ_R^2 , and $\chi_{\sigma_R}^2$ allow us to observe the quality of the fit separately for each observable. The

f_i 's are free normalization parameters. In order to produce a statistically meaningful quantity we also calculated the χ^2 per degree of freedom (χ_ν^2). The minimum search with up to 33 parameters required a fast minimizing routine. From among the standard routines the one based on the Marquart algorithm¹⁷ proved to be the most efficient. The derivatives with respect to the fitting parameters were calculated analytically, which reduced the computer time by a factor of 5.

B. The data base

The input data for the present analysis are given in Table II. A few comments are necessary for σ_R .

(i) The datum at 52 MeV required a small correction,

TABLE II. Data base for the PSA.

E_p (MeV)	Number of data points; reference for			R
	$d\sigma/d\Omega$	A_y	σ_R (mb)	
30.35	51; 2	20; 1	70±9;18	
32.15	54; 2	20; 1	73±8;18	
34.25	48; 2	20; 1	82±7;18	
36.90	53; 2	20; 1	95±7;18	
39.75	62; 2	19; 1	105±6;18	
45.0	80; 2	22; 4	109±6;18	
52.3	41; 4	41; 4	112±7 ^b	
59.6	37; 4	37; 4	111±8 ^b	
64.9	41; 4	41; 4	110±8 ^b	11; 5
71.9	44 ^a	44 ^a	108±10 ^b	

^aThis paper.

^bDerived as described in the text.

since the value given in Ref. 19 did not include reactions contributing to the very forward and backward hemispheres. The correction was estimated assuming an isotropic angular dependence for the (p,pn) and the (p,pnp) differential cross sections and using the (p,d) differential cross section at 49.5 MeV (Ref. 20). As a result the value increased from (107.7 ± 4.4) mb to (111.7 ± 7.0) mb.

(ii) To obtain σ_R at higher energies we extrapolated from the lower-energy data using the energy dependence of the n - ^4He total reaction cross section. This in turn was derived from the n - ^4He total cross section²¹ by subtracting the total elastic cross section. For the region of overlap the total reaction cross sections for n - ^4He and p - ^4He agree within statistics. The errors of the extrapolated values were set rather high in order to account for the low-energy normalization errors and the energy dependence uncertainty. In comparison to the extrapolated σ_R values used by Ref. 3, our values are about 10% lower for $E \geq 55$ MeV.

The statistical weight for σ_R was taken to be that of just one data point. This is in contrast to, e.g., Ref. 1, where σ_R was arbitrarily given weights corresponding to two or eight data points. Reference 2 tested different weights but observed essentially to influence on the PS.

C. Single-energy analysis

In order to test our search routine, we started at 30 MeV with Plattner's solution as a starting set. Partial waves were restricted identically to $l \leq 4$. As expected, the Plattner solution was essentially reproduced between 30 and 40 MeV. When we investigated the χ^2 function with starting values further off the Plattner solution, we, however, found new solutions with χ^2 values, which are lower by 30 to 50%. It should be noted that Plattner's solution was fixed in the sense that the $^2D_{3/2}$ PS up to 32 MeV was given by an R -matrix calculation, which restricted the flexibility of the fit. We shall show herein that indeed the $^2D_{3/2}$ PS exhibits the biggest uncertainty and, hence, a constraint on $^2D_{3/2}$ has a large effect on the other PS.

Since multiple solutions with comparable χ^2 were found at all other energies as well, we studied this phenomenon by using artificial data: a set of 60 $d\sigma/d\Omega$

and 60 A_y data points—also including σ_R —was created, which were randomly distributed with realistic errors around the prediction of the best-fit PS solution at 45 MeV. These data were then subjected to a PSA ($l \leq 5$), which yielded several solutions with comparable χ^2 . When we reduced the errors, some of these solutions disappeared or acquired larger χ^2 values. However, even with unrealistically small errors, i.e., $\sim 0.05\%$ for $d\sigma/d\Omega$ and ~ 0.001 for A_y , two solutions remained: the input solution A and another solution (called B). Both solutions had almost identical χ^2 values, but differed by at least 10% in most PS. Evidently the large number of fit parameters and their correlation does not allow for a unique PS determination on the basis of $d\sigma/d\Omega$ and A_y alone, almost irrespective of their uncertainties. The problem could be solved by an accurate measurement of R at backangles, as is demonstrated in Fig. 2. Although the difference between both predictions is largest around 120° , an accuracy of $\Delta R \simeq 0.10$ around 60° would be enough to discriminate between both curves.

We conclude, that a unique PS determination by using the criterion of the lowest χ^2 value is impossible, unless one has some *a priori* knowledge on some of the PS. We cannot decide whether the energy dependence of the PS is truly smooth or not. Hence, we made the plausible assumption of smoothness, and in the cases where there were several solutions with comparable χ^2 values, we selected the ones which yielded a more smooth energy dependence.

Owing to the complicated character of the χ_{tot}^2 hypersurface around the minima the statistical uncertainty of the PS could not be determined directly from the diagonal elements of the corresponding error matrix (cf. e.g., Ref. 22). Instead we proceeded in the following way: a given PS was changed step by step—with the other PS adjusted so as to minimize the χ_{tot}^2 —until χ_{tot}^2 increased by 1. As a rule, the largest deviation of a PS from its value at the minimum, corresponding to a χ_{tot}^2 increase of 1 was used to define the error, regardless of which PS was

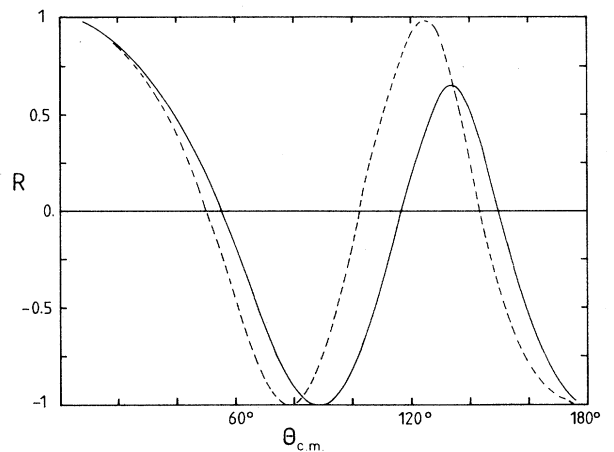


FIG. 2. Phase-shift predictions for the spin rotation parameter R at 45 MeV. The solid line results from the input solution A , whereas the dashed line represents solution B as mentioned in the text.

TABLE III. Single-energy PS and related quantities between 30 and 45 MeV.

PS	30.35 MeV		32.15 MeV		34.25 MeV		36.9 MeV		39.75 MeV		45.0 MeV	
	$\delta(^{\circ})$	η	$\delta(^{\circ})$	η	$\delta(^{\circ})$	η	$\delta(^{\circ})$	η	$\delta(^{\circ})$	η	$\delta(^{\circ})$	η
$^2S_{1/2}$	76.99	0.950	75.93	0.956	74.03	0.973	70.19	0.953	70.03	0.898	63.72	0.780
$^2P_{3/2}$	79.20	1.0	79.13	0.928	73.38	1.0	70.67	1.0	67.20	1.0	65.55	1.0
$^2P_{1/2}$	42.93	0.992	45.72	1.0	42.50	0.994	39.98	0.987	35.97	0.995	30.31	0.963
$^2D_{5/2}$	16.04	0.857	18.15	0.886	15.31	0.839	17.57	0.809	17.52	0.762	22.20	0.677
$^2D_{3/2}$	4.427	0.815	6.145	0.803	6.974	0.680	6.040	0.706	7.846	0.651	8.213	0.691
$^2F_{7/2}$	6.129	0.960	7.356	0.962	7.593	0.963	8.949	0.912	10.54	0.907	12.84	0.863
$^2F_{5/2}$	4.314	1.0	5.903	0.973	6.952	0.955	7.098	0.936	7.773	0.938	8.157	0.913
$^2G_{9/2}$	0.506	0.992	0.661	0.996	0.634	0.989	0.619	0.982	0.983	0.977	2.287	0.976
$^2G_{7/2}$	0.014	0.966	-0.076	0.977	0.271	0.959	-0.282	0.956	-0.090	0.945	-0.273	0.954
$^2H_{11/2}$											0.247	1.0
$^2H_{9/2}$											0.431	0.998
σ_R	74.96		75.73		89.20		102.31		110.44		118.50	
f_{σ}	0.9893		0.9752		0.9811		0.9855		0.9947		1.0072	
f_A	1.0001		1.0019		1.0002		1.0004		1.0005		0.9962	
χ_{σ}^2	0.372		0.530		0.670		0.411		0.675		0.473	
χ_A^2	0.548		0.315		0.431		0.754		1.037		1.003	
$\chi_{\sigma R}^2$	0.304		0.116		1.059		1.091		0.821		2.509	
χ_{tot}^2	0.422		0.624		0.615		0.518		0.769		0.607	
χ_{ν}^2	0.563		0.821		0.832		0.684		0.977		0.772	

actually investigated. Since the χ_{tot}^2 function around the minimum was often not symmetric, upper and lower bounds were obtained independently.

The errors attach the proper statistical significance to a given solution and are very useful when comparing different solutions at the same energy or when studying the energy dependence of single PS. One could also use

them to study the sensitivity of a given PS to specific observables.

Our final PS are given in Tables III and IV, together with the values for σ_R , the normalization factors f_i , and the various χ^2 values defined earlier. The PS as a function of energy are shown in Fig. 3 together with the results of the Plattner/Houdayer and Saito(1) solutions.

TABLE IV. Single-energy PS and related quantities between 52 and 72 MeV.

PS	52.3 MeV		59.6 MeV		64.9 MeV "O"		64.9 MeV "R"		71.9 MeV	
	$\delta(^{\circ})$	η	$\delta(^{\circ})$	η	$\delta(^{\circ})$	η	$\delta(^{\circ})$	η	$\delta(^{\circ})$	η
$^2S_{1/2}$	49.46	0.765	47.75	0.754	44.22	0.805	48.67	0.741	43.00	0.761
$^2P_{3/2}$	59.57	1.0	57.45	0.838	54.62	0.820	51.94	0.910	53.32	0.743
$^2P_{1/2}$	25.29	1.0	26.14	0.993	23.98	0.974	18.50	0.985	21.19	0.926
$^2D_{5/2}$	29.62	0.607	29.16	0.615	29.64	0.693	28.36	0.640	29.13	0.665
$^2D_{3/2}$	8.761	0.667	8.687	0.710	8.339	0.756	11.45	0.728	7.961	0.769
$^2F_{7/2}$	15.30	0.847	15.81	0.870	15.45	0.847	15.96	0.828	14.78	0.829
$^2F_{5/2}$	7.121	0.878	6.458	0.875	6.407	0.801	7.381	0.810	5.678	0.765
$^2G_{9/2}$	2.948	1.0	4.017	0.987	5.068	0.950	4.602	0.987	5.569	0.957
$^2G_{7/2}$	0.279	0.930	0.397	0.920	0.350	0.912	0.793	0.930	0.852	0.914
$^2H_{11/2}$	-0.270	1.0	0.382	1.0	0.503	0.993	1.686	0.993	1.170	0.996
$^2H_{9/2}$	1.177	0.971	1.336	0.980	2.225	0.958	1.178	0.974	2.126	0.961
$^2I_{13/2}$							0.227	1.0		
$^2I_{11/2}$							0.293	0.987		
$^2J_{15/2}$							-0.483	0.989		
$^2J_{13/2}$							0.003	0.985		
σ_R	117.26		110.33		114.02		114.41		111.40	
f_{σ}	0.9901		1.0002		1.0004		1.0033		1.0016	
f_A	1.000		1.0000		0.9989		0.9995		1.0112	
f_{rot}							0.9814			
χ_{σ}^2	0.912		0.639		0.867		0.848		0.606	
χ_A^2	0.863		0.786		0.830		0.861		0.819	
χ_R^2							1.820			
$\chi_{\sigma R}^2$	0.565		0.007		0.253		0.211		0.115	
χ_{tot}^2	0.890		0.780		0.841		0.944		0.707	
χ_{ν}^2	1.210		1.103		1.146		1.376		0.940	

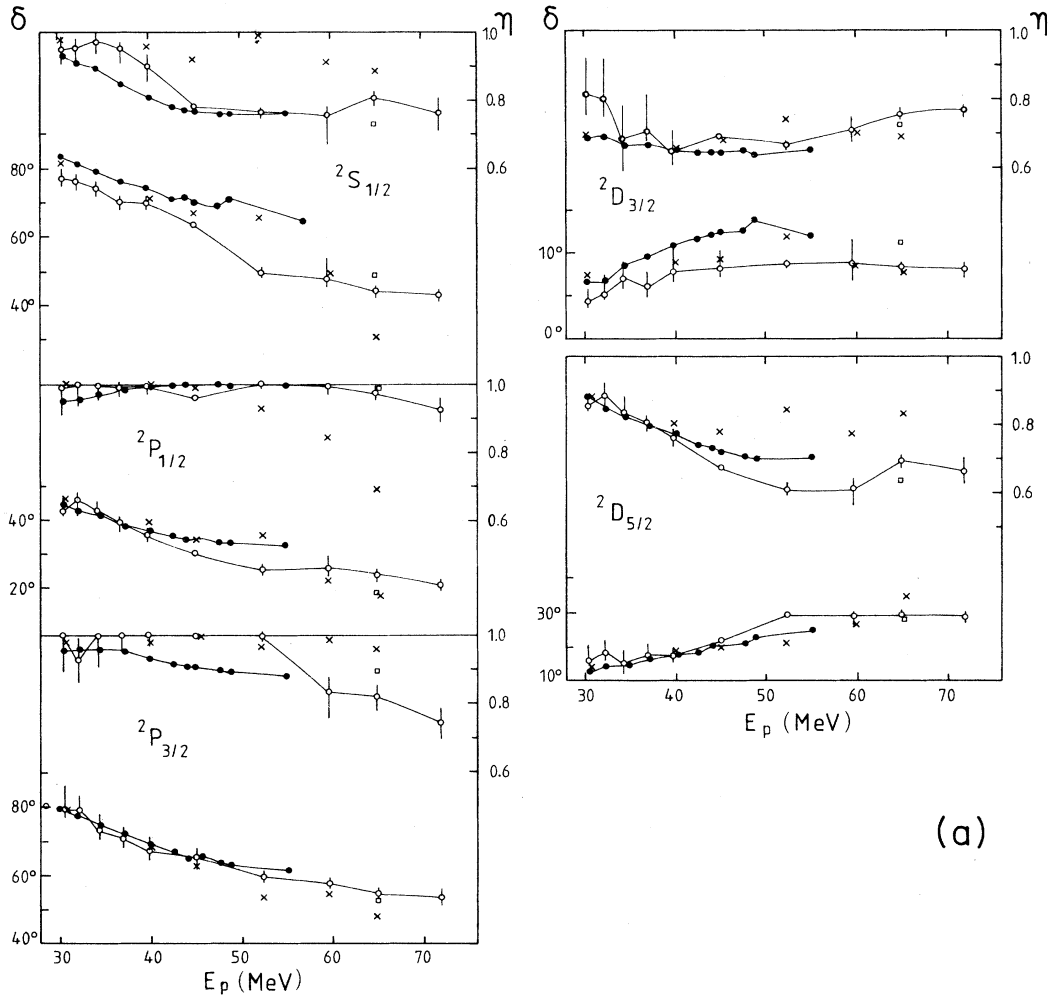


FIG. 3. (a) Energy dependence for the S , P , and D phase shifts of Ref. 2 (solid dots), solution 1 of Ref. 3 (crosses) and of this work (open circles with error bars). The solutions of Ref. 2 as well as ours are connected by a solid line to guide the eye. At 65 MeV the squares represent the solution "R," which includes the spin rotation data. The left scale refers to the real part (δ) of the PS, whereas the right scale refers to the imaginary part (η). (b) The energy dependence for the F , G , and H phase shifts. For explanation of the details refer to (a).

D. Energy dependent analysis

In order to study the energy dependence of the PS more rigorously, we performed an energy dependent analysis, where the PS were constrained to follow a certain energy dependence. This dependence is *a priori* not known. However, since our single-energy PS seem to follow a simple energy dependence, we proceeded empirically and expanded the PS up to second order in E :

$$\begin{aligned}\delta_l(E) &= \delta_{l,0} + \delta_{l,1} \times E + \delta_{l,2} \times E^2, \\ \eta_l(E) &= \eta_{l,0} + \eta_{l,1} \times E + \eta_{l,2} \times E^2,\end{aligned}\quad (5)$$

with $l=0, 1, \dots, 5$.

In the analysis, 645 data points were fitted. The 45 MeV data were rejected because they increased the χ^2_{tot} out of proportion. In order to treat all energies on the

same footing, the R data were also omitted. The $d\sigma/d\Omega$ and A_y data were not renormalized as in the single-energy searches, because the normalization factors acquired unrealistic values.

The final PS usually go—within the errors—through the single-energy solutions. For some parameters however, significant differences are observed and as a result the χ^2_{ν} amounts to the very high value of 13.2. The reason for the high χ^2_{ν} is probably the simple-energy parametrization: the PS have to be correlated very precisely to produce the low χ^2_{ν} , and even small deviations from the values at the minimum increase the χ^2_{ν} considerably. The simple parametrization does not allow us to fulfill this subtle correlation requirement. On the other hand, the PS of the single-energy analysis deviate sometimes from a smooth interpolation curve and pushing them onto the curve leads to a high χ^2_{ν} .

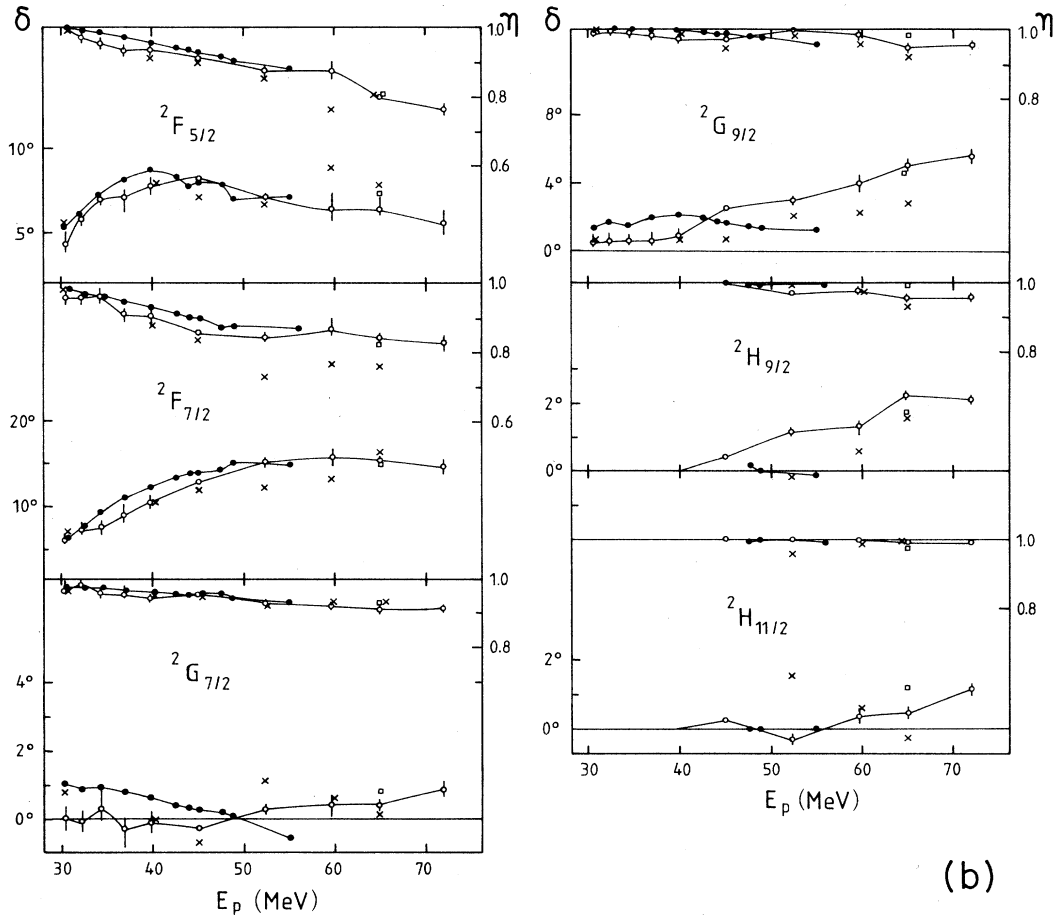


FIG. 3. (Continued).

E. Discussion

We shall first comment on the results at specific energies.

We have already discussed the origin of the small differences between the Plattner solution and ours below 40 MeV. Using Houdayer's more extensive cross section data had essentially no influence on the PS, while the errors were reduced by typically 20%. Given the size of our error bars, it appears meaningless to assign any significance to the small structures in some of the PS around 30 MeV, as has been done tentatively by Refs. 1 and 2.

At 45 MeV we initially used the same data base as Saito and, similarly, could not find a solution with $\chi_v^2 \leq 2.0$ ($l \leq 5$). After introducing the extensive cross section data of Ref. 2, the χ_v^2 fell below 1 for several minima. Given this situation we decided to select a PS set which does not represent a true minimum, but provides a smooth energy dependence. No errors could be calculated however.

At 52 and 65 MeV the effect of including forward angle A_y data is clearly visible from the size of the errors, as compared to 59 or 72 MeV.

At 65 MeV we studied the impact of back-angle spin rotation data by comparing the solutions with (called solution "R") and without (called solution "O") R data

(cf. Table IV and Fig. 3). Whereas in the latter case our solution described the data well ($\chi_v^2 = 1.15$), the best "R" solution found had $\chi_v^2 = 2.3$. It was only after including higher partial waves ($l \leq 7$) that the χ_v^2 dropped to the reasonable value of 1.38 (the R data are still not very well described: $\chi_R^2 = 1.8$).

The influence of partial waves with $l=6,7$ can in fact be expected from the $l=kr$ rule, since already at about 23 MeV $l=4$ contributions become important.^{1,2} The complete set of observables allowed a unique determination even with the inclusion of $l=6,7$ contributions. The unique solution "R" is very similar to the "O" solution, which was selected according to our usual criteria. This indicates, that our solutions at 59 and 72 MeV also must be close to the "true" ones and provides further support for our selection philosophy.

At 72 MeV the significance of including σ_R was tested: without σ_R the χ_{tot}^2 was more or less constant over a wide range of PS values, whereas with σ_R several clear minima appeared. This behavior emphasizes the importance of including this particular observable, although it represents only one out of 89 data point at that energy. Qualitatively this sensitivity is apparent from the definition of σ_R , which involves only squares of the inelastic parameters η_l , whereas the other observables also include interference terms between different PS and the

sensitivity to certain PS may vanish. The PS predictions for $d\sigma/d\Omega$ and A_y are shown in Fig. 1.

On the whole, our solutions exhibit an energy dependence which is smooth and in the region of overlap similar to the ones of Plattner/Houdayer. Concerning the comparison with Saito, it should be noted that we could reproduce, essentially, all of his solutions. The observed differences are due to the fact that our selection criteria were not only a statistically proper χ^2_ν , but also a smooth energy dependence. Whether the latter assumption is justified or not cannot be decided with the present data. There are indications in the literature that any high-lying excitations of ^5Li —if they exist at all—should be broad, overlapping levels.^{1,2} Hence, the elastic p - ^4He scattering would be best described by smoothly varying PS.

IV. CONCLUSIONS

The aim of the present investigation was to study the energy dependence of the PS in p - ^4He elastic scattering between 30 and 72 MeV. We approached this goal via a single energy and an energy dependent procedure. In the single-energy analysis we found—similarly to Ref. 3—several solutions with comparable χ^2 values at all energies. Analyzing artificial data, we could show definitely that these solutions are equivalent, if only $d\sigma/d\Omega$ and

A_y data (almost irrespective of their accuracy) are available. As a consequence the true energy dependence of the PS cannot be determined unambiguously without additional data (the spin rotation parameter at back angles) or further constraints on the PS. Based on the plausible assumption that the PS above 30 MeV should be smoothly varying, a set of such solutions was found. The new solutions typically exhibit smaller or at least comparable χ^2_ν values than existing ones. The statistical uncertainties of the PS, which were derived from the shape of the χ^2 hypersurface near the minima themselves, revealed that they are consistent with a smooth energy dependence. In view of these uncertainties, it appears meaningless to assign any significance to the small structures in some of the PS around 30 MeV, as has been done tentatively by Refs. 1 and 2. The energy dependent analysis confirmed the trend of the single-energy analyses. However, the χ^2_ν is large, which is due to the strong correlation of the PS in connection with the constraint that the energy dependence of the PS follows a curve of second order.

We greatly appreciate the help of Dr. D. Eversheim, Dr. F. Hinterberger, J. Doberitz, and B. von Przewoski during data takings as well as fruitful discussions with Dr. G. R. Plattner.

*Present address: Department of Physics and Astronomy, University of Kentucky, Lexington, KY 40506.

¹G. R. Plattner, A. D. Bacher, and H. E. Conzett, *Phys. Rev. C* **5**, 1158 (1972).

²A. Houdayer, N. E. Davison, S. A. Elbakr, A. M. Sourkes, W. T. H. van Oers, and A. D. Bacher, *Phys. Rev. C* **18**, 1985 (1978).

³T. Saito, *Nucl. Phys.* **A331**, 477 (1979).

⁴K. Imai, K. Hatanaka, H. Shimizu, N. Tamura, K. Egawa, K. Nisimura, T. Saito, H. Sato, and Y. Wakuta, *Nucl. Phys.* **A325**, 397 (1979).

⁵H. Togawa, H. Sakaguchi, M. Nakamura, K. Imai, M. Yosoi, M. Ieiri, Y. Takeuchi, T. Tsutsumi, T. Nakano, S. Hirata, T. Saito, T. Ichihara, and S. Kobayashi, Research Center for Nuclear Physics, Osaka University, Annual Report, 1985.

⁶R. Henneck, C. Gysin, M. Hammans, J. Jourdan, W. Lorenzon, M. A. Pickar, I. Sick, S. Burzynski, and T. Stambach, *Nucl. Instrum. Methods* **A259**, 329 (1987).

⁷J. Fröhlich, H. Kriesche, L. Streit, and H. Zankel, *Nucl. Phys.* **A384**, 97 (1982).

⁸H. Zankel, private communication.

⁹E. A. Silverstein, *Nucl. Instrum. Methods* **4**, 53 (1959).

¹⁰J. F. Janni, *At. Data Nucl. Data Tables* **27**, 147 (1982).

¹¹R. A. Arndt, Programme SAID.

¹²J. N. Palmieri, A. M. Cormack, N. F. Ramsey, and R. Wilson, *Ann. Phys. (N.Y.)* **5**, 299 (1958).

¹³Young and L. H. Johnston, *Phys. Rev.* **119**, 313 (1960).

¹⁴W. Haeberli, R. Henneck, C. Jaquemart, J. Lang, R. Müller,

M. Simonius, W. Reichart, and C. Weddigen, *Nucl. Instrum. Methods* **163**, 403 (1979).

¹⁵M. Ieiri, H. Sakaguchi, M. Nakamura, H. Sakamoto, H. Ogawa, M. Yosoi, T. Ichihara, N. Isshiki, Y. Takeuchi, H. Togawa, T. Tsutsumi, S. Hirata, T. Nakano, S. Kobayashi, T. Noro, and H. Ikegami, *Nucl. Instrum. Methods* **A257**, 253 (1987).

¹⁶R. C. Hanna, in *Proceedings of the 2nd International Symposium on Polarization Phenomena of Nucleons, Karlsruhe, 1965*, edited by P. Huber and H. Schopper (Birkhauser, Stuttgart, Germany, 1966).

¹⁷Marquardt algorithm, P. R. Bevington, *Data Reduction and Error Analysis for the Physical Sciences* (McGraw-Hill, New York, 1969), p. 235.

¹⁸A. M. Sourkes, N. E. Davison, S. A. Elbakr, J. L. Horton, A. Houdayer, W. T. H. van Oers, and R. F. Carlson, *Phys. Lett.* **51B**, 232 (1974); A. M. Sourkes, A. Houdayer, W. T. H. van Oers, R. F. Carlson, and R. E. Brown, *Phys. Rev. C* **13**, 451 (1976).

¹⁹D. J. Cairns, T. C. Griffith, G. J. Lush, A. J. Metheringham, and R. A. Thomas, *Nucl. Phys.* **60**, 369 (1964).

²⁰S. A. Harbison, R. J. Griffith, N. M. Stewart, A. R. Johnston, and G. T. A. Squier, *Nucl. Phys.* **A152**, 503 (1970).

²¹D. F. Measday and J. N. Palmieri, *Nucl. Phys.* **85**, 129 (1966); B. Hänsler *et al.*, *Phys. Rev. C* **28**, 995 (1983); P. Hillman, R. H. Stahl, and N. F. Ramsey, *Phys. Rev.* **96**, 115 (1954).

²²R. A. Arndt, R. H. Hackman, and L. D. Roper, *Phys. Rev. C* **15**, 1021 (1977).